High-power efficient diode-pumped $Nd{:}YVO_4/LiB_3O_5$ 457 nm blue laser with 4.6 W of output power

Q. H. Xue, Q. Zheng, Y. K. Bu, F. Q. Jia, and L. S. Qian

Changchun Institute of Optics, Fine Mechanics and Physics, Chinese Academy of Sciences, Changchun Jilin, 130033, China, and Graduate School of the Chinese Academy of Sciences, Beijing 100080, China

Received November 16, 2005; revised January 9, 2006; accepted January 13, 2006; posted January 25, 2006 (Doc. ID 66075)

Continuous-wave 457 blue laser emission at powers as high as 4.6 W is achieved by using a fiber-coupled laser diode array with a power of 30 W to pump 0.1 at. % low-doped bulk $Nd{:}YVO_4$ crystal, with intracavity frequency doubling in a 15 mm long type I critical phase-matched LiB_3O_5 (LBO) crystal in a compact threefold cavity with a length of less than 100 mm. The optical–optical conversion efficiency is greater than 15.3%, and the stability of the output power is better than 3% for an hour. © 2006 Optical Society of America

OCIS codes: 140.3480, 140.3580.

There has been great interest in multiwatt level blue laser emission for applications such as underwater communications, high-density optical storage, and medical diagnostics, especially for color display technologies.[1–3] A laser-diode- (LD) pumped solid-state quasi-three-level Nd^{3+} laser has proved to be an efficient way to achieve this goal.[4,5]

Fan and Byer[4] first successfully demonstrated the operation of a LD-pumped quasi-three-level Nd:YAG laser that operates on the $^4F_{3/2} \rightarrow {}^4I_{9/2}$ transition, and they founded the corresponding theoretical model. Thereafter, Risk[5] established a similar model to describe this kind of laser. An important conclusion can be drawn from these theoretical models: that is, the quasi-three-level system can be regarded as a four-level structure once the intracavity fundamental wave circulating intensity is high enough that the reabsorption loss is bleached. When this point is reached, the laser will either come into a benign operational state and a higher optical conversion efficiency will be expected, or the laser will come into the opposite state. Overcoming these problems, a 2.8 W 473 nm $Nd{:}YAG/BiB_3O_6$ (BIBO) laser and an 840 mW 456 nm $Nd{:}GdVO_4/LiB_3O_5$ (LBO) laser were demonstrated with a Z cavity as long as almost 1 m.[2,3] A 2.0 W, 457 nm doubling-frequency $Nd{:}YVO_4$ thin disk has been reported,[6] and 1.0 W is available commercially.[7]

As candidates for blue lasers, $Nd{:}YVO_4$ and $Nd{:}GdVO_4$ crystals have several advantages over Nd:YAG crystal, including higher absorption cross sections, wider absorption bandwidths, and polarized output. The linearly polarized laser output is favorable not only to nonlinear frequency conversion but also to avoiding undesired birefringent effects. $Nd{:}YVO_4$ and $Nd{:}GdVO_4$ have similar thermal populations of about 5% at room temperature according to their crystal field splittings of 433 and 409 cm^{-1}, respectively.[2] Although $Nd{:}GdVO_4$ has better thermal conductivity than $Nd{:}YVO_4$, the thermal-induced dioptic power (the reciprocal of the thermal lens) is a function of thermal conductivity, the thermo-optic coefficient, and the thermal expansion coefficient, which leads to a comparable thermal lens for $Nd{:}YVO_4$.[8,9]

In this Letter a high-power, compact, efficient cw 457 nm blue laser based on fiber-coupled LD-pumped intracavity frequency-doubling $Nd{:}YVO_4$/LBO is demonstrated. With an incident pump power of 30 W, low-doped bulk $Nd{:}YVO_4$, a long type I phase-matched LBO crystal, and a compact, three-mirror folded cavity, up to 4.6 W of blue laser emission at 457 nm is achieved. The optical–optical conversion efficiency is greater than 15.3%, and the stability of the output power is better than 3% for an hour.

The experimental setup of the intracavity-doubled 457 nm $Nd{:}YVO_4$/LBO blue laser is shown in Fig. 1. The pump source is a 30 W 808 nm fiber-coupled LD array with a core diameter of 400 μm and a numerical aperture of 0.22 for cw pumping. Its emission's center wavelength is 806 nm at 25 °C and can be tuned by changing the temperature of the heat sink to match the best absorption of the laser crystal. The coupling optics consists of two identical plano–convex lenses with focal lengths of 10 mm used to reimage the pump beam into the laser crystal at a ratio of 1:1. The coupling efficiency is 98%. Because the pump intensity is high enough in the pump spot regions, the first lens must be well adjusted to collimate the pump beam, since it will strongly affect the focal spot. However, the distance between the two lenses can be freely adjusted by experiment. For the aberration, the average pump spot radius ω_p is around 220 μm. The laser crystal is a 5 mm length of $Nd{:}YVO_4$ crystal doped with 0.1 at. % $Nd{:}^{3+}$. Its left side is coated with antireflection films at the pump wavelength

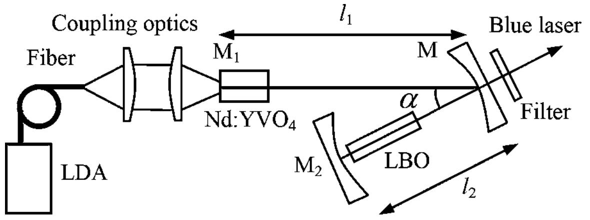

Fig. 1. Setup for the intracavity frequency-doubled 457 nm $Nd{:}YVO_4$/LBO blue laser.

($R<2\%$) and with high-reflection films at 914 nm ($R>99.9\%$), acting as one mirror (M_1) of the cavity. A low-doped, long laser crystal is advantageous to reduce thermal lensing and the reabsorption of quasi-three-level emission while guaranteeing that enough pump energy will be absorbed. When the pump wavelength is tuned to match the absorption peak of the $\mathrm{Nd:YVO_4}$, a pump power of about 60% is absorbed. The crystal is wrapped with indium foil and mounted in a copper holder cooled through the resonator base plate, which is kept at a constant temperature of 15 °C by a thermoelectric cooler, which helps to yield a small thermal population of the terminal laser level and stable output power. The lower temperature is essential to yield efficient operation at the $\mathrm{Nd:YVO_4}$ spectral line of 914 nm. When the coating requirements on the left-hand side of the $\mathrm{Nd:YVO_4}$ are satisfied, measurement indicates that reflections at 1064 and 1342 nm are 80% and 30%, respectively. The right-hand side of the laser crystal is antireflection coated at 914, 1064, and 1342 nm to reduce loss of the resonating 914 nm light and suppress the strong 1064 and 1342 nm lines that can oscillate parasitically with the left-hand side.

A folded plano–concave mirror (M) with a small radius of curvature ($R=50$ mm) is adopted to reduce the length of the system. The concave surface is high-reflection coated at 914 nm ($R>99.8\%$) and high-transmission coated at 457, 1064, and 1342 nm. The coating films for the plane surface are the same as for the right-hand side of the $\mathrm{Nd:YVO_4}$, except with high transmission at 457 nm. The end mirror (M_2) with a radius of curvature of 300 mm is high-reflection coated at 914 nm ($R>99.8\%$) and 457 nm ($R>99\%$), providing double reflection of the second-harmonic wave.

Optimization of the coupling output of the intracavity doubling-frequency laser can be realized by changing the length of the same nonlinear crystal, as discussed by Smith.[10] Type I critical phase-matching 10 and 15 mm long LBO crystals ($\theta=90°$, $\varphi=21.7°$ at 300 K) are tested to the double frequency 914 nm.

Two arms constitute the folded three-mirror resonator. One is the collimating arm (l_1), which has a larger beam radius (ω_1) in $\mathrm{Nd:YVO_4}$, and the other is the focusing arm (l_2), which has a smaller beam waist radius (ω_{02}) in LBO. Note that the geometric length of the cavity must be replaced by the physical length so that the lengths of the crystals can be compared with the compact cavity length. The physical lengths of the two arms are $L_1=l_1-(l_{\mathrm{Nd}}-l_{\mathrm{Nd}}/n_e)$ and $L_2=l_2-(l_{\mathrm{LBO}}-l_{\mathrm{LBO}}/n_o)$, respectively, where l_{Nd} and l_{LBO} are the geometric lengths of $\mathrm{Nd:YVO_4}$ and LBO; $n_e=2.175$ and $n_o=1.608$ are the refractive indices of the extraordinary ray in $\mathrm{Nd:YVO_4}$ and the ordinary ray in LBO. When the mechanical structures are in place, the beam's incident angle ($\alpha/2$) upon the folded mirror is set to be as small as possible ($\approx 5°$) to reduce the astigmatism without additional optical astigmatism-compensating elements.

Only about 18 W is absorbed from the 30 W of incident power. The thermal-lens focal length is estimated to be 200 mm, equivalent to a curved mirror with the same numerical value on the end of the cavity.[11] The long thermal lens, even under the conditions of high pump power and tight focusing, is attributed to a small quantum defect of 12%. This is beneficial for thermal-lens compensation by resonator design. Because the beam quality factor M^2 of a real laser is usually greater than 1, an *ABCD* matrix formalism including M^2 (assuming 2) is introduced to study the dynamic operation of the compact, folded three-mirror resonator.[12]

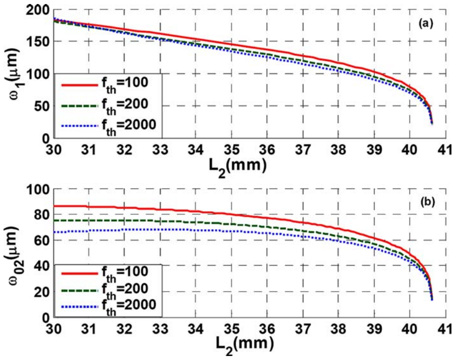

Fig. 2. (Color online) Average beam radii in $\mathrm{Nd:YVO_4}$ and LBO as a function of the physical length of the second arm. (The parameter is the thermal-lens focus length. $M^2=2$, $L_1=65$ mm).

As α is very small, numerical calculation shows that the differences between tangential and sagittal beam radii in $\mathrm{Nd:YVO_4}$ and LBO are only 2 and 0.5 μm, respectively. Ignoring the astigmatism, as shown in Fig. 2 the average beam radii in the middle of $\mathrm{Nd:YVO_4}$ and LBO are nearly constant over a broad region of thermal-lens focus lengths, from near infinity down to 100 mm, given the length of the second arm. Different thermal-lens focus lengths do not affect the stable region of the cavity. There is about 10 mm that can be adjusted for the second arm length. However, we should notice that a ±1 mm change of the second arm will decrease or increase the radius of ω_1 by 10 μm, while the effect on ω_{02} is not so serious. Therefore the second arm must be adjusted with care in the experiments. When the pump power is increased, in order to maintain the same parameters of the cavity in the laser and nonlinear crystals as those for lower pump powers, one has to lengthen the second arm slightly, although the resonator is a thermally stable one. Using the physical length of the first arm as the parameter, as shown in Fig. 3, L_1 has little effect on ω_1 when $L_2=34$ mm. But the longer the first arm, the smaller the stable region determined by the second arm.

When the laser medium, nonlinear crystal, and the cavity are given, a different length of the nonlinear crystal changes the output coupling of the laser power as a different reflection mirror of fundamental wave would. In the experiments 10 and 15 mm LBO crystals are used. At maximum pump power, 3.3 and 4.6 W of 457 nm blue light are obtained, respectively. The output power as a function of the input power is shown in Fig. 4. Note that the parameters are all optimized at 30 W of pump power. A high lasing threshold (about 12 W) seems the reverse of the thermal stable resonator stated above; however, there is another phenomenon that is like a step response in Fig. 4 (at 18 W). The reasons for these characteristics are attributed to the saturation of reabsorption loss of the quasi-three-level laser for the fundamental wave of 914 nm. At lower pump powers, a lower circulating intensity exists in the cavity, and the corresponding high reabsorption loss leads to a high threshold. As the pump power increases, the circulating intensity becomes so high that it bleaches the reabsorption loss, and the output power increases suddenly.[1] The laser will operate like a four-level system after this turning point, for the reabsorption loss is approaching zero. Thereafter, the system operates as the usual intracavity doubling-frequency laser. During the experiments, when the temperature of the pump source is turning to match the absorption peak of $Nd:YVO_4$ at every incident power, the threshold and the turning point are lower than the data shown in Fig. 4. However, the trend is the same.

The beam quality factor M^2 is measured to be about 2.5 by the knife-edge technique,[13] which is consistent with the analysis of the resonator. A stability of better than 3% for an hour is measured by a FieldMaster-GS powermeter.

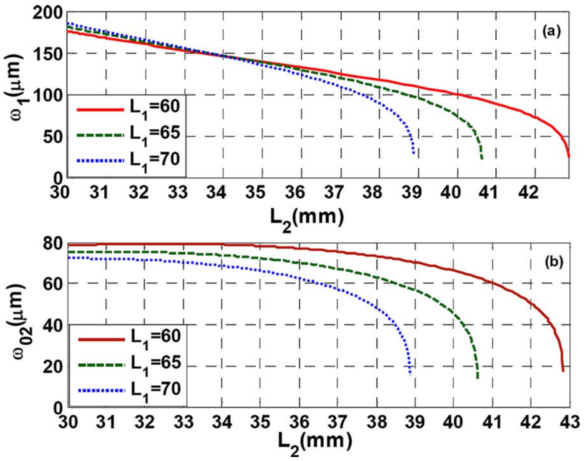

Fig. 3. (Color online) Average beam radii in $Nd:YVO_4$ and LBO as a function of the physical length of the second arm. (The parameter is the physical length of the first arm. $M^2=2$, $f_{\mathrm{th}}=200$ mm).

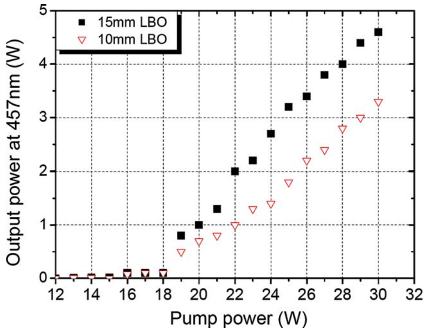

Fig. 4. (Color online) Output power at 457 nm as a function of the pump power at 808 nm.

However, by measuring the 457 nm leakage from the long arm of the resonator, the noise of the blue laser is observed with a silicon fast photodiode by the filtered fundamental wave and pump light. This is due to cross saturation in the laser crystal and sum-frequency mixing in the doubling-frequency crystal.[14] In our experiments, although no method, such as changing the polarization state of 914 nm or forcing operation at a single frequency, is adopted to overcome this problem, low noise is observed for a few minutes when the gap between the end mirror and the LBO is adjusted carefully because the internally reflected blue laser at the mirror has a significant effect on phase locking and elimination of noise through parametric processes.[15]

In summary, a high-power, compact, efficient cw 457 nm blue laser based on a fiber-coupling laser-diode-pumped intracavity frequency-doubling $Nd:YVO_4/LBO$ crystal is demonstrated successfully. With an incident pump power of 30 W, low-doped bulk $Nd:YVO_4$, a long type I phase-matching LBO crystal, and a compact three-mirror folded cavity, up to 4.6 W of blue laser emission at 457 nm is achieved. The optical–optical conversion efficiency is greater than 15.3%, and the stability of the output power is better than 3% for an hour.

Q. H. Xue's e-mail address is xueqinghua001 @126.com.

References

1. P. Zeller and P. Peuser, Opt. Lett. **25**, 34 (2000).
2. C. Czeranowsky, M. Schmidt, E. Heumann, G. Huber, S. Kutovoi, and Y. Zavartsev, Opt. Commun. **205**, 361 (2002).
3. C. Czeranowsky, E. Heumann, and G. Huber, Opt. Lett. **28**, 432 (2003).
4. T. Y. Fan and R. L. Byer, IEEE J. Quantum Electron. **23**, 605 (1987).
5. W. P. Risk, J. Opt. Soc. Am. B **5**, 1412 (1988).
6. A. Schlatter, L. Krainer, M. Golling, and R. Paschotta, Opt. Lett. **30**, 44 (2005).
7. www.lasersystem.de.
8. M. Okida, M. Itoh, T. Yatagai, H. Ogilvy, J. Piper, and T. Omatsu, Opt. Express **13**, 4909 (2005).
9. N. W. Rimington, S. L. Schieffer, W. Andreas Schroeder, and B. K. Brickeen, Opt. Express **12**, 1426 (2004).
10. R. G. Smith, IEEE J. Quantum Electron. **6**, 215 (1970).
11. B. Neuenschwander, R. Weber, and H. P. Weber, IEEE J. Quantum Electron. **31**, 1082 (1995).
12. P. A. Belanger, Opt. Lett. **16**, 196 (1991).
13. A. E. Siegman and S. Johnston, Jr., IEEE J. Quantum Electron. **27**, 1098 (1991).
14. T. Baer, J. Opt. Soc. Am. B **3**, 1175 (1986).
15. M. Tsunekane, N. Taguchi, and H. Inaba, Opt. Lett. **22**, 1000 (1997).